

# Indoor aerosol dynamics, composition, and pathway-specific biological responses in human bronchial epithelial cells (BEAS-2B) at Rome Fiumicino International Airport (OASIS Project\*).

Massimo Santoro<sup>1</sup>, Maria Pierdomenico<sup>1</sup>, Laura Caiazzo<sup>1</sup>, Lorenzo De Silvestri<sup>1</sup>, Angelica Scamarcia<sup>2</sup>, Costanza Messeri<sup>2</sup>, Liudmila Dobriakova<sup>3</sup>, Francesco Cuscito<sup>3</sup>, Milena Stracquadano<sup>1</sup>, Teresa Maria Giovanna La Torretta<sup>1</sup>, Ettore Petralia<sup>1</sup>, Ilaria D'Elia<sup>1</sup>, Giandomenico Pace<sup>1</sup>, Fabio Spaziani<sup>1</sup>, Marco Proposito<sup>1</sup>, Maria Giuseppa Grollino<sup>1</sup>, Antonio Piersanti<sup>1</sup>, Barbara Benassi<sup>1</sup>.

<sup>1</sup>ENEA-Italian National Agency for New Technologies, Energy and Sustainable Economic Development, Rome, Italy.

<sup>2</sup>BU Healthy Reply, Santer Reply S.r.l., Turin, Italy.

<sup>3</sup>BU Concept Reply, Santer Reply S.r.l., Turin, Italy



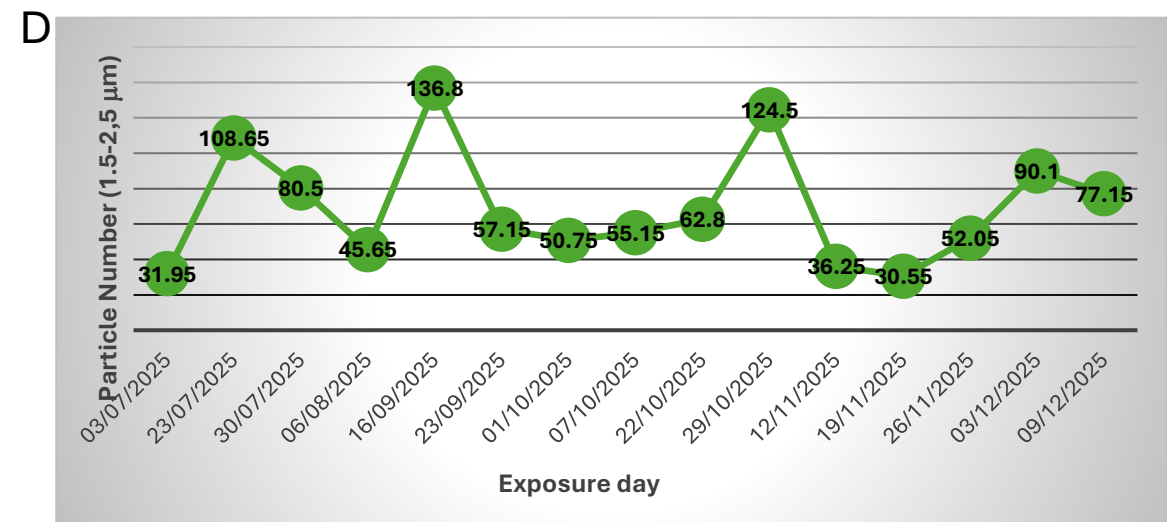
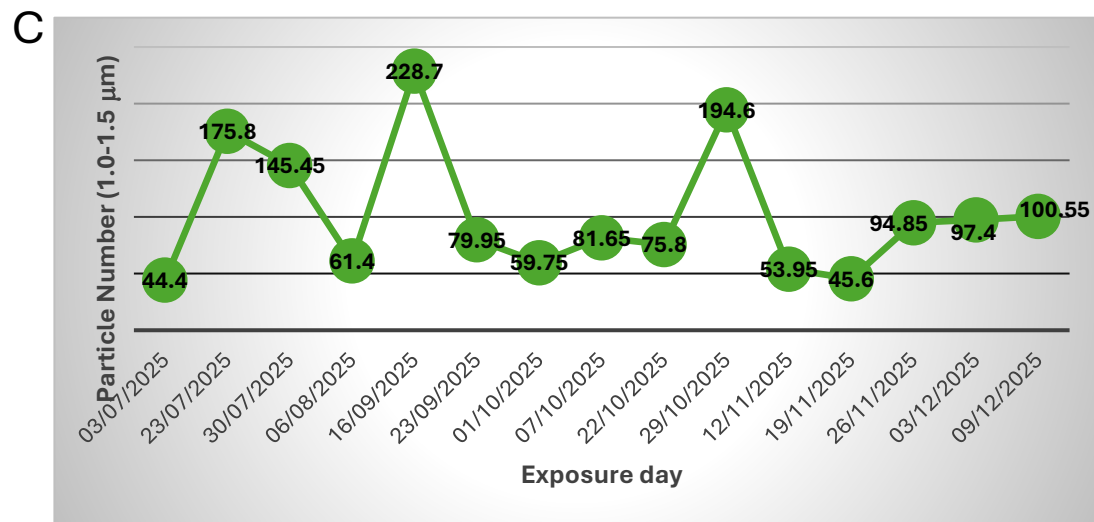
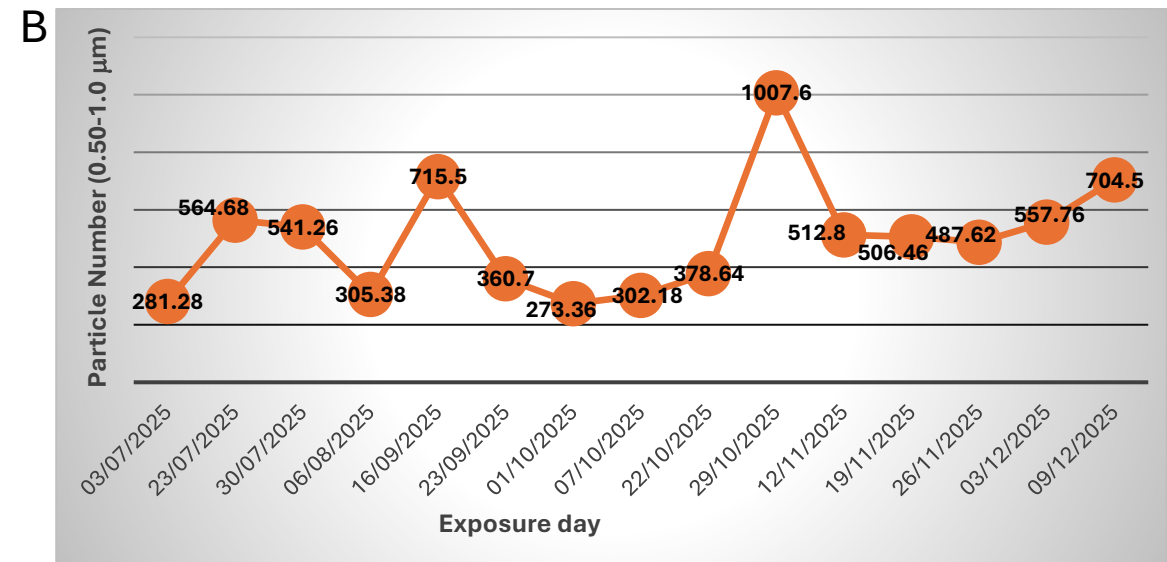
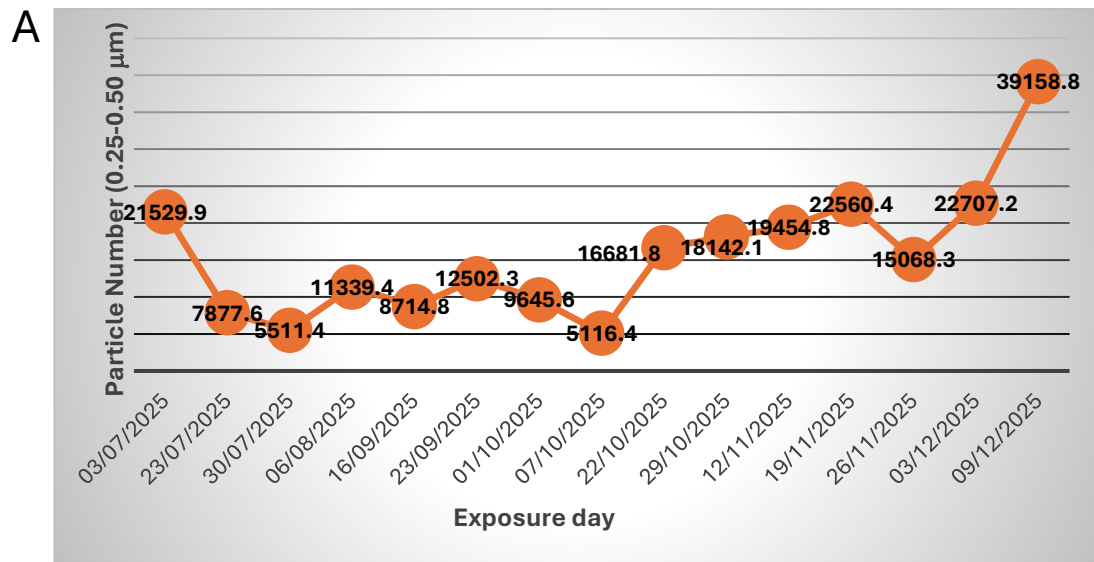


**Figure 1.** The figure illustrates how particle number concentrations evolved across four particulate matter (PM) size ranges during 15 exposure sessions carried out between July and December 2025. Panel A shows the smallest particles (0.25–0.50  $\mu\text{m}$ ), which display pronounced variability, including several sharp rises and a marked increase toward the end of the monitoring period. Panel B (0.50–1.0  $\mu\text{m}$ ) reveals a pattern of recurring peaks and dips, suggesting episodic events influencing this size fraction. In Panel C (1.0–1.5  $\mu\text{m}$ ), the particle counts fluctuate with intermittent spikes that interrupt otherwise lower baseline levels. Finally, Panel D (1.5–2.5  $\mu\text{m}$ ) presents a more moderate but still oscillating trend, with alternating high and low values that persist throughout the exposure timeline. Together, the four panels highlight the dynamic and size-dependent nature of particle number variations over the study period.

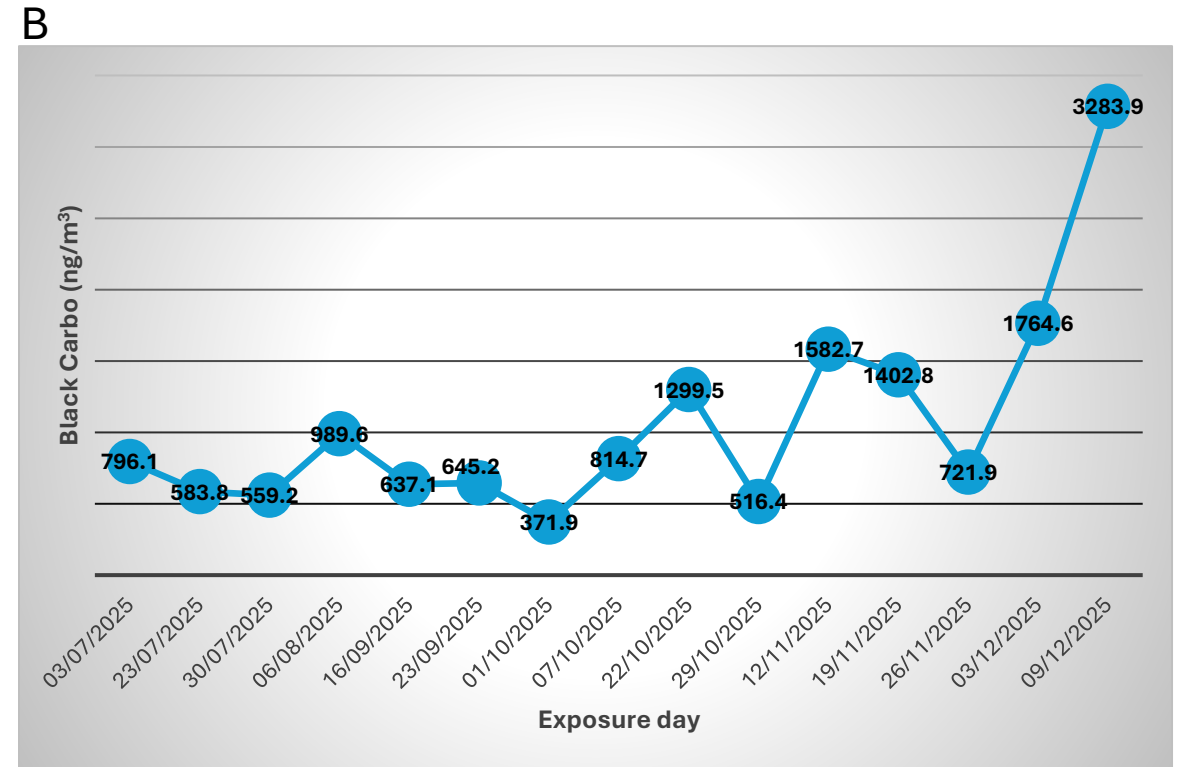
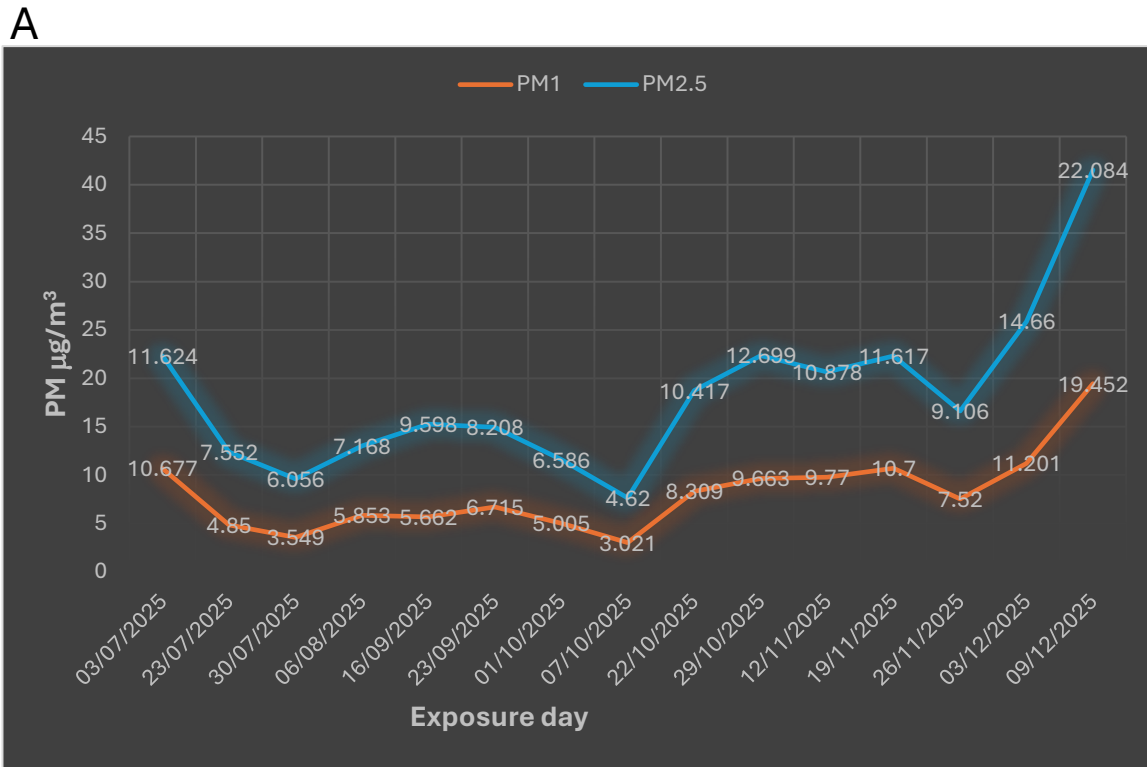


**Figure 2.** This figure illustrates how concentrations of particulate matter and black carbon evolved over the course of 15 exposure days from July to December 2025. In Panel A, the two curves representing PM<sub>1</sub> and PM<sub>2.5</sub> reveal a dynamic pattern that unfolds gradually over the monitoring period. During the summer and early autumn exposures, both fractions fluctuate within a relatively contained range, with PM<sub>2.5</sub> consistently remaining above PM<sub>1</sub>. These early variations suggest alternating periods of cleaner and slightly more polluted conditions. As the timeline progresses toward late autumn and early winter, the curves begin to rise more noticeably. The final exposure days show a clear and sharp increase in both PM<sub>1</sub> and PM<sub>2.5</sub>, indicating a substantial shift in particulate levels, likely driven by seasonal changes or intensified emission sources. Panel B mirrors this story through the lens of black carbon (BC) concentrations. For much of the monitoring period, BC levels oscillate moderately, with occasional peaks that quickly return to baseline. However, as with the particulate mass data, the final part of the timeline is marked by a dramatic surge. This pronounced rise in BC aligns closely with the late-season increase observed for PM<sub>1</sub> and PM<sub>2.5</sub>, pointing toward a shared underlying cause—such as increased combustion-related emissions or meteorological conditions that favor pollutant accumulation. Together, the two panels provide a coherent picture of how air quality evolved across the study period, highlighting a distinct escalation in pollutant levels as winter approached.

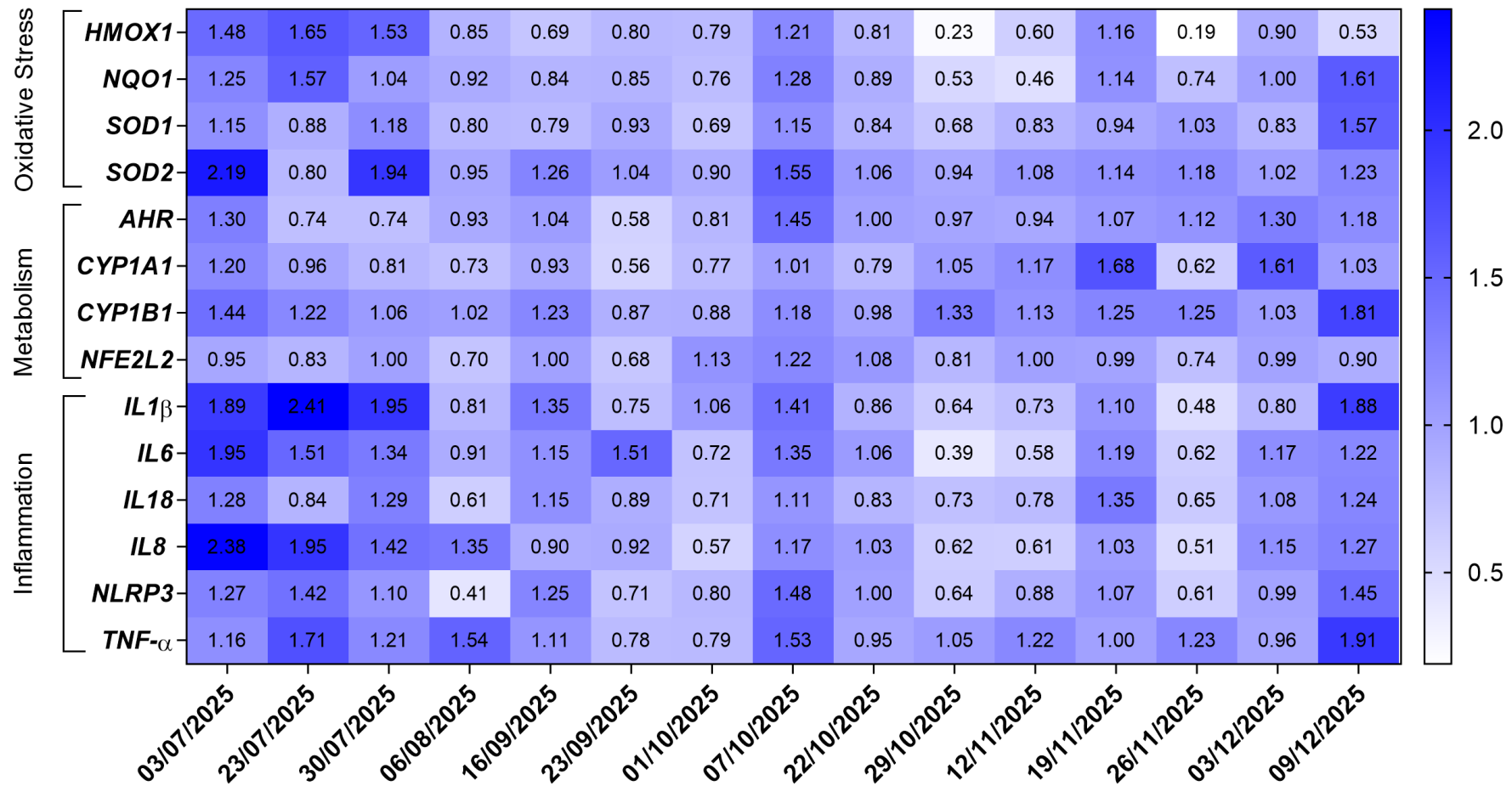


**Figure 3.** Heat map showing how the expression of selected genes changed over time during exposure sessions conducted from July to December 2025. The map is based on the fold change of each gene, meaning how much its activity increased or decreased compared to a reference level. Genes are grouped into three functional categories: oxidative stress, metabolism, and inflammation. Each column represents one exposure day; darker colors indicate higher fold-change values, while lighter colors reflect lower expression. Genes associated with oxidative stress (*HMOX1*, *NQO1*, *SOD1*, *SOD2*) show varying degrees of modulation, with some periods marked by elevated expression, suggesting episodic activation of antioxidant defense mechanisms. The metabolic genes (*AHR*, *CYP1A1*, *CYP1B1*, *NFE2L2*) display distinct temporal patterns, with certain dates showing stronger induction, potentially reflecting fluctuations in xenobiotic sensing and detoxification pathways. In the inflammatory gene cluster (*IL1 $\beta$* , *IL6*, *IL18*, *IL8*, *NLRP3*, *TNF- $\alpha$* ), expression levels vary considerably across the exposure days. Some genes exhibit intermittent peaks, indicating transient inflammatory responses, while others remain relatively stable or show gradual increases toward the later dates. Overall, the heat map highlights dynamic, pathway-specific shifts in gene expression across the study period, revealing how different biological processes were differentially engaged from July to December 2025.